Journal of Power Sources 195 (2010) 3529–3535

Contents lists available at ScienceDirect

Journal of Power Sources

journal homepage: www.elsevier.com/locate/jpowsour

Fabrication of metallic bipolar plate for proton exchange membrane fuel cells by rubber pad forming

Yanxiong Liu, Lin Hua*

School of Automobile Engineering, Wuhan University of Technology, Luoshi Road 122#, Wuhan 430070, China

ARTICLE INFO

Article history:
Received 10 December 2009
Accepted 10 December 2009
Available online 21 December 2009

Keywords:
Metallic bipolar plate
Rubber pad forming
Micro-scale flow channel
Fuel cell
Finite element simulation

ABSTRACT

In this paper, the rubber pad forming process is used to fabricate the metallic bipolar plate for a proton exchange membrane (PEM) fuel cell, which has multi-array micro-scale flow channels on its surface. The rubber pad forming process has the following advantages: high surface quality and dimensional accuracy of the formed parts, low cost of the die because only one rigid die is required, and high efficiency. The process control parameters (rubber hardness, internal and outer radii, draft angle) of the rubber pad forming are analyzed by the finite element method using the commercial software Abaqus. After that, the rubber pad forming process is used to manufacture a metallic bipolar plate of SS304 stainless steel with perfect flow micro-channels. The results of this effort indicated that the rubber pad forming process is a feasible technique for fabricating the bipolar plates of PEM fuel cells.

1. Introduction

In recent years, there has been great interest from governments and research institutions in proton exchange membrane (PEM) fuel cells due to their high efficiency, fast startup, and potential for energy conservation, safety, and environmental protection. The PEM fuel cell is the main candidate for replacing the internal combustion engine in transportation applications [1,2]. However, the current cost of a fuel cell is 4–10 times greater than an internal combustion engine (PEM fuel cell: \$200–30 kW^{-1}, internal combustion engine: \$30–50 kW^{-1}). Of all the different components of the fuel cell, the bipolar plate is the largest bottleneck for the commercialization of the PEM fuel cells because its weight is 60–80% of the stack weight and its cost is 30–45% of the stack cost [3,4]. The U.S. Department of Energy (DOE) has set a goal of lowering the overall cost of the bipolar plate to \$6 kW^{-1} by the year 2010.

Nowadays, there are three main types of bipolar plates: (1) graphite bipolar plates, (2) polymer–carbon composite bipolar plates, and (3) metallic bipolar plates. Metallic bipolar plates have received considerable attention due to their low cost, excellent mechanical, electrical, and thermal properties, and their ease of production [5–7]. Parallel to the development of a corrosion resistant metallic material, it is also necessary to develop an efficient and cost effective fabrication process of the bipolar plate in order to make the production of metallic bipolar plates commercially viable.

The primary difficulty in manufacturing a metallic bipolar plate is the formation of the micro-channel. In the past few years, several fabrication methods of the metallic bipolar plate have been developed. Koc and Mahabunphachai [8] developed a manufacturing process involving internal pressure-assisted embossing of the micro-channels with in-die mechanical bonding. Lee and Lee [9] fabricated micro-scaled flow channels by electrochemical micro-machining. Yokoyama et al. [10] studied fabrication by hot pressing in the supercooled liquid state. However, the fabrication process using internal pressure-assisted embossing of micro-channels with in-die mechanical bonding is not suitable when the anode and cathode plates are not symmetrical. In addition, hydroforming and mechanical bonding are difficult to perform in a single production set up, and experiments investigating the hydroforming and mechanical bonding were carried out separately as the authors presented in their paper. The surface quality of the parts formed by electrochemical micro-machining is poor, and this method is inefficient. A die with high heat resistance is required for the hot pressing method, and the productivity for this method is also low.

This paper presents a novel method for producing a metallic bipolar plate for use in PEM fuel cells: the rubber pad forming process, which adopts a rubber pad contained in a container acting as a rigid die. The rubber pad forming process has many advantages over the traditional sheet fabrication process using rigid die set [11]. The new method only utilizes one rigid die, and the lower die is a rubber pad. The contact surface between the rigid die and the rubber is flexible, which greatly improves the formability of the blank to be shaped. Only one rigid die must be manufactured, and the rubber pad and rigid die do not need to be assembled precisely. Therefore, the

* Corresponding author. Tel.: +86 27 87168391; fax: +86 27 87168391.
E-mail addresses: liuyx716@163.com, lhuasvs@yahoo.com.cn (L. Hua).

0378-7753/$ – see front matter © 2009 Elsevier B.V. All rights reserved.
doi:10.1016/j.jpowsour.2009.12.046

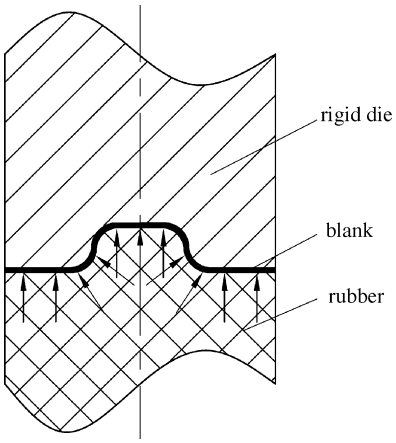

Fig. 1. Schematic diagram of the rubber pad forming process.

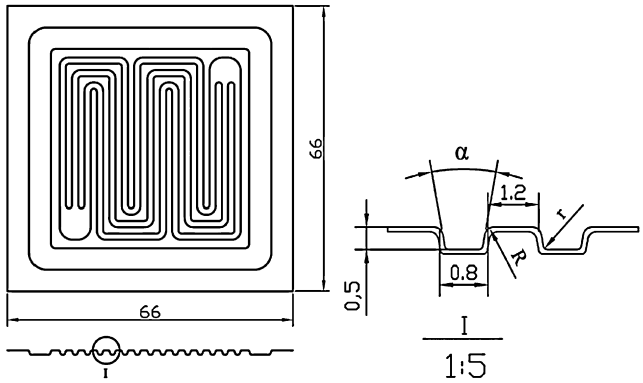

Fig. 2. Schematic diagram of the bipolar plate sample.

time and cost required for the forming equipment can be greatly reduced.

Former researchers have investigated the rubber pad forming process. Browne and Battikha [12] described a rubber pad process for manufacturing an aircraft wing or tail flap. Dirikolu and Akdemir [13] investigated the significant parameters associated with the rubber pad forming process using numerical method. They determined that the rubber hardness, advance, blank material type, contact friction, and die design are crucial parameters that require adjustment before production. Thiruvarudchelvan [14] presented several kinds of flexible processes to produce sheet metal ashtrays and plates. Salau [15] optimized the process with numerical simulations and experiments. Ramezani et al. [16] studied the friction behavior of the rubber pad forming process. In these studies, attention has been concentrated on the deformation of large parts, but the forming process deforms differently during the fabrication of micro-parts such as micro-channels [17].

In this paper, finite element analysis (FE, Abaqus/Standard software) is used to analyze the rubber pad forming process. The main process parameters such as the rubber hardness and the key geometric dimensions of the rigid die (the draft angle α, outer radius R, and internal radius r) are explored with the FE model. A metallic bipolar plate is also fabricated and tested by a 3D laser scanning system.

2. Principles of the rubber pad forming process

The rubber pad forming process is ideal for forming microchannels. Fig. 1 shows a schematic diagram of the forming process [11]. As the rigid die moves down, the rubber deforms elastically and provides a counter-pressure. Then, because of the counter-pressure, the rubber and the blank flow into the cavity of the rigid die together. The fabrication process can be divided into two steps: (1) drawing the blank to the bottom of the rigid die using the counter-pressure of the rubber pad, and (2) filling the blank until it fits the rigid die.

A bipolar plate sample is designed as shown in Fig. 2. The thickness of the bipolar plate is 0.1 mm, and the shape of bipolar plate channel is snake-liked. The dimensions of the bipolar plate channels affect the reaction efficiency of the fuel cell and play an important role in the formability of the blank. According to the studies of Watkins et al. [18], Peng et al. [19], and others, the geometric dimensions of the micro-channel include the outer fillet radius (R), internal fillet radius (r), draft angle (α), flow channel depth (h = 0.5 mm), flow channel width (w = 0.8 mm), and rib width (s = 1.2 mm).

The equipment for the rubber pad forming is designed to manufacture the metal bipolar plate as shown in Fig. 3. The equipment is composed of five parts: the rigid die, the stainless steel sheet, the rubber pad, the steel container enclosing the rubber pad, and the fastening plate fixing the container. Polyurethane rubber with a Shore A hardness of 70 (HD70) is used as a pad, and a SS304 annealed stainless steel sheet with a thickness of 0.1 mm is applied. Because much time and effort are required to manufacture the rigid die with various geometries, FE simulation is adopted as the major tool to investigate the effect law of the process parameters in this study.

3. Finite element modeling

The bipolar plate is not symmetrical (Fig. 2) and would ideally be simulated by a 3D FE model. However, numerical simulations of the rubber pad forming process are complicated because the method involves coupling of the deformation of the blank and rubber. Because of the large deformation of the rubber pad, a severe mesh distortion may occur, which would lead to loss of precision and even termination of the simulation. In order to save time and improve the computational precision, a 2D FE model is used. The three micro-scaled flow channels that are made in the bipolar plate sample (Fig. 2) are analyzed as one cycle in the 2D FE model (Fig. 4).

3.1. Material model

The rigid die is defined as an analytical rigid body and no material properties need to be specified. Therefore, only two different materials are included in the FE model: a hyper-elastic material to describe the rubber pad and an elastic–plastic model of the blank.

In this study, polyurethane rubber is used as the rubber pad. The behavior of the nonlinear hyper-elastic and incompressible rubber-like material is usually described by the Mooney–Rivlin model,

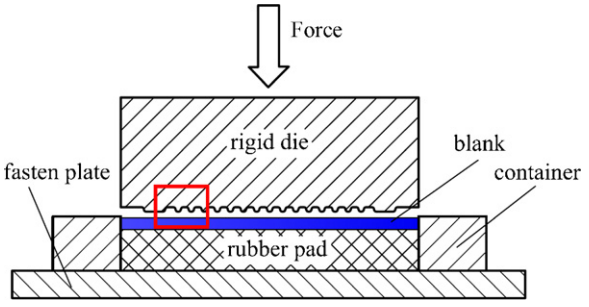

Fig. 3. Sketch of the equipment used for bipolar plate fabrication by the rubber pad forming.

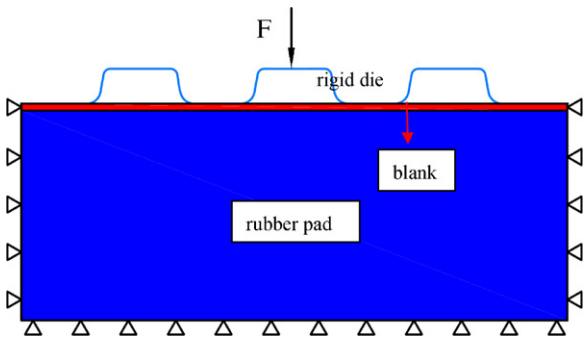

Fig. 4. 2D finite element model.

which uses a strain energy function W. The derivative of W with respect to a strain component determines the corresponding stress component. The strain energy can be expressed by the following function [20]:

$$\sigma_{ij} = \frac{\partial W}{\partial \varepsilon_{ij}}$$
$$W = \sum_{k+m=1}^{n} C_{km}(I_1 - 3)^k + (I_2 - 3)^m + \frac{1}{2}k(I_3 - 1)^2 \quad (1)$$

where I_1, I_2, and I_3, are the strain invariants, k is the bulk modulus, and C_{km} is the constant of the Mooney–Rivlin material model. For incompressible materials, $I_3 = 1$. In this study, two-parameters (C_{10} and C_{01}) of the Mooney–Rivlin model are used to describe the polyurethane rubber pad material behavior, and $n = 1$.

To investigate the effect of the rubber hardness on plate fabrication, two kinds of rubber (HD55 and HD70) are used in the FE model. The mechanical properties of the rubber pads are listed in Table 1.

An SS304 annealed stainless steel sheet with a thickness of 0.1 mm is used as the blank. The stress–strain curve is obtained from tensile tests of the annealed SS304. Five tensile specimens conforming to GB-T228-2002 are tested (Fig. 5). The mean value of the curves used in the FE model is shown in Fig. 6. The elasticity module (E) and Poisson's ratios (ν) of the annealed SS304 are 162.5 GPa and 0.3, respectively. And the constitutive relation of annealed SS304 in the tensile plastic deformation can be obtained by the method of curve fitting and linear regression as Eq. (2):

$$\sigma = (799.9\varepsilon^{0.232} + 60.9)\,\text{MPa} \quad (2)$$

where σ and ε are the true stress and true strain, respectively.

3.2. Finite element mesh

In the rubber pad forming process, the rigid die is treated as an analytical rigid body. Four-node bilinear plane strain with quadrilateral reduced and integration hourglass control elements (CPE4R) are applied to model the stainless steel blank. Four-node bilinear plane strain quadrilateral hybrid elements with reduced integration and hourglass control (CPE4RH) are applied to describe the rubber pad. Hybrid element is incompressible and suitable to represent the rubber-liked material property [21].

Table 1
Mechanical properties of the rubber pads [20].

Polyurethane rubber	Hardness shore A	M–R constant C_{10} (MPa)	M–R constant C_{01} (MPa)	Poisson's ratio (ν)
Type 1	55	0.382	0.096	0.4999
Type 2	70	0.736	0.184	0.4999

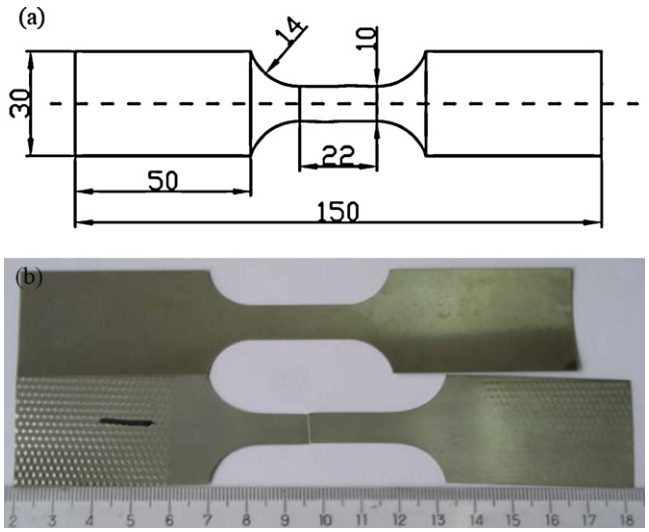

Fig. 5. (a) Dimensions of the annealed SS404 stainless steel specimen and (b) photos of the specimens before and after the tensile test.

3.3. Dynamic contact conditions

There are two different contact pairs in the rubber pad forming process: between the surface of the rigid die and the upper surface of the blank and between the lower surface of the blank and the upper surface of the rubber pad. Both pairs are surface-to-surface contacts and allow a small amount of sliding between the surfaces. The frictional behavior of both contact pairs is assumed to follow Coulomb's model. Under lubricated conditions, the friction coefficient is 0.2 for the first pair and 0.1 for the second pair [20].

3.4. Constraint and load

The rubber pad is fixed in the container during the forming process. In order to simplify the simulation model, the container is not considered in this model through adding constraint on the rubber pad. The lower surface of the rubber is held fixed in all directions, and the sides of the rubber surface are fixed in the x-direction and are free in the y-direction. The rigid die is only allowed to move in the y-direction. Translation of the rigid die can be controlled by a concentrated force, F, which is the load force in this model.

A detailed geometry of the rigid die and the specific process conditions used in the FE model are summarized in Table 2.

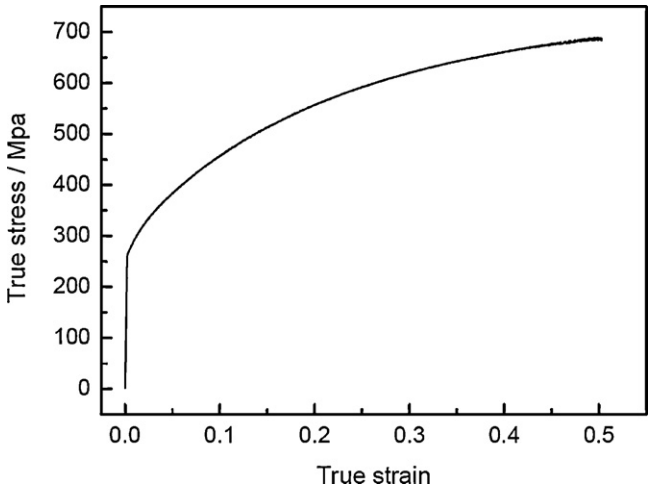

Fig. 6. Stress–strain curve of the annealed stainless steel SS304.

Table 2
Dimensional information for the FE model and specifications of the fabrication process employed in this study.

Dimensions of the FE model (mm)	
Rigid die	
$H = 0.5$ $s = 1.2$ $W = 1.0$ $\alpha = 5^\circ/10^\circ/15^\circ/20^\circ$ $R = 0.1/0.2/0.3$ $r = 0.1/0.2$ ($R + r \leq H$)	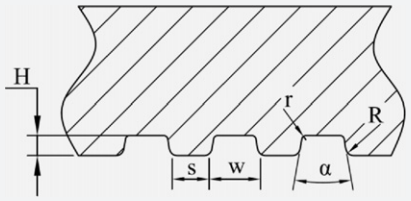
Load force (kN)	100/250

3.5. Verification of the simulation model

To verify the accuracy of the FE simulation, the fracture surface morphology of a bipolar plate formed using the rubber pad forming process is compared with the results of the FE simulation. Both in the simulation and the experiment, the dimensions of the rigid die R, r, and α are 0.2, 0.2, and 20°, respectively, and the load force F is 250 kN.

Fig. 7 shows the bipolar plate formed by the experiment and the FE simulation. The plate is cut in the middle along the dotted line. In order to observe the fracture, the profile of the plate is projected and enlarged to 100 times using optical measurement equipment (Fig. 7a). The plate is cracked at the corner of the rib of the micro-channels. Fig. 7b shows the surface of the plate predicted by the FE simulation. The stress is concentrated at the corners of the micro-channels, and the thickness in these locations is reduced,

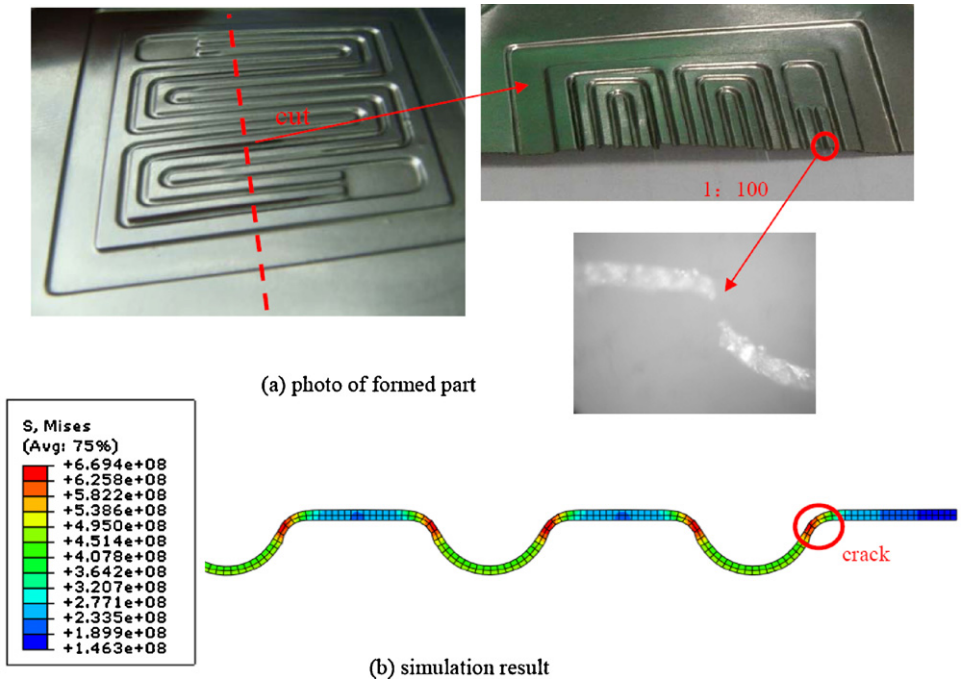

Fig. 7. The bipolar plate formed by the experiment and the FE simulation.

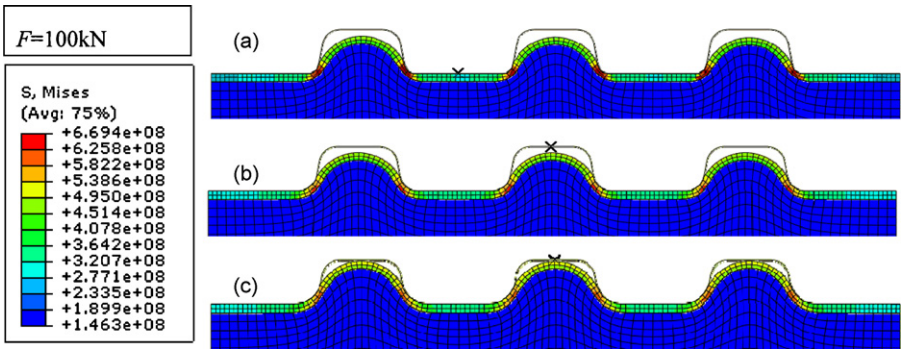

Fig. 8. Simulated micro-channels with $\alpha = 20^\circ$ and different radii: (a) $R = 0.1$, $r = 0.2$; (b) $R = 0.2$, $r = 0.2$; (c) $R = 0.3$, $r = 0.2$.

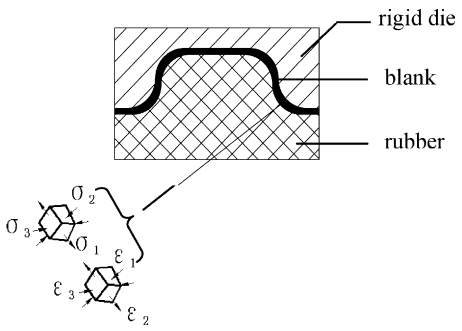

Fig. 9. Stress and strain state at the corner of a micro-channel.

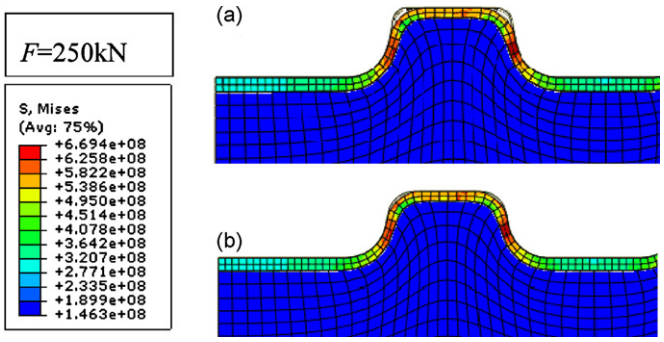

Fig. 10. Fabricated plates with $\alpha = 20^\circ$ and different internal radii: (a) $R = 0.3$, $r = 0.1$; (b) $R = 0.3$, $r = 0.2$.

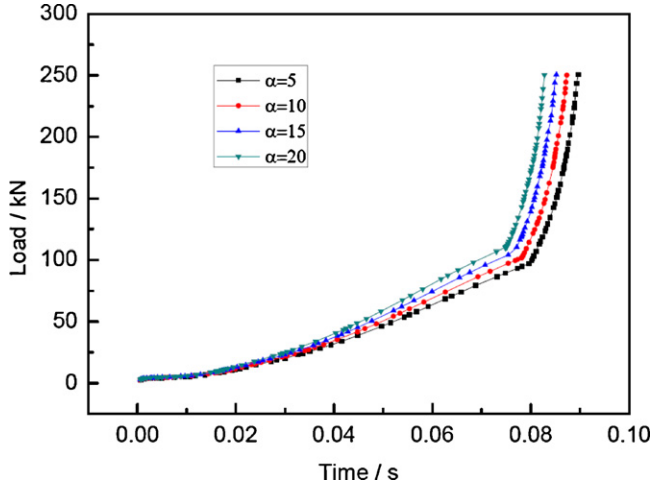

Fig. 11. Forming load with the time increment at various draft angles α of the rigid die.

leading to cracking. The FE simulation agreed well with experimental results and could be used to investigate the effect of other process parameters on deformation.

3.6. Simulation results

3.6.1. Effect of outer radius R and internal radius r

In the rubber pad forming process, the radii of the rigid die played an important role in determining the formability of the blank. A simulation is performed with a constant internal radius ($r = 0.2$), a rubber pad of HD70, a load force $F = 100$ kN, and an outer radius R that varied from 0.1 to 0.3 mm. As R increased, the filling percentage of the blank increased (Fig. 8). When R is 0.2 or 0.1, the channels might be cracked at the corners, but an outer radius of 0.3 mm appeared to lead to a stable plate. This can be explained by Fig. 9.

Fig. 9 represents the stress and strain states at the corner of the micro-channel during deformation. It shows that plate not only suffers from tensile stress σ_1 in the radial direction, but also from stress σ_3 in the tangential direction and the stress σ_2 due to the blending pressure imposed by the rigid die [22]. The smaller the value of R, the larger the blending pressure imposed by the rigid die will be. The sheet metal may bend seriously and fail to fill the cavity of the rigid die if the outer radius is too small.

To investigate the effect on plate deformation, r is changed from 0.1 mm to 0.2 mm, with R held constant at 0.3 mm ($r + R \leq 0.5$). Fig. 10 shows the formed plates at different fillet radii for the forming load $F = 250$ kN. When $r = 0.1$ mm, the blank does not fill the rigid die completely, and the filling percentage is perfect $r = 0.2$ mm. Therefore, the smaller r is, the more difficult it is to fill the cavity of the rigid die.

3.6.2. Effect of the draft angle α

To investigate the effect on the rubber pad forming process, the draft angle α is changed from 5° to 20° for $R = 0.3$ mm, $r = 0.2$ mm, and $F = 250$ kN. In these models, all of the blanks filled the rigid die completely, but the variation curves of these forming loads with the time increment are different. Fig. 11 shows the forming load with the time increment at various draft angles. The time required for the blank to fill the cavity of the rigid die decreased as α increased. Therefore, larger values of α is beneficial for the rubber pad forming process.

3.6.3. Effect of rubber hardness

To analyze the effect of the rubber hardness on the deformation of the plate, two rubber pads of different Shore A hardness (Table 1) are used in the FE model. The key parameters are $R = 0.3$ mm, $r = 0.2$ mm, $\alpha = 20^\circ$, and $F = 250$ kN. As shown in Fig. 12, the filling percentages of the micro-channels are perfect regardless of the hardness of the rubber pads. Fig. 12 also shows that the Von-Mises stress distributions of the formed plates are almost the same in the stress concentrated region. The hardness of the rubber pad is not

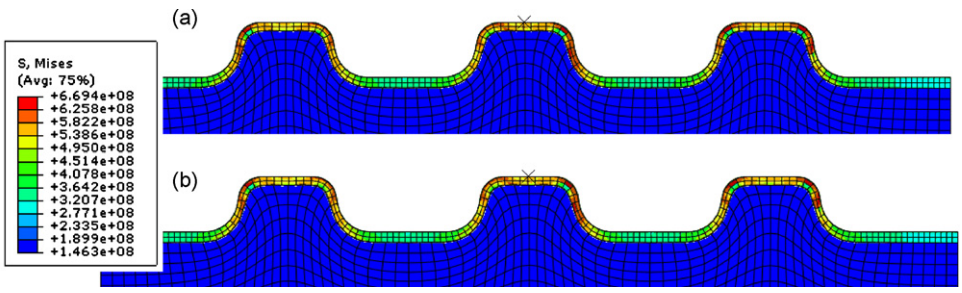

Fig. 12. The formed parts at different rubber pad (250 kN): (a) rubber pad with Shore A hardness of 55; (b) rubber pad with Shore A hardness of 70.

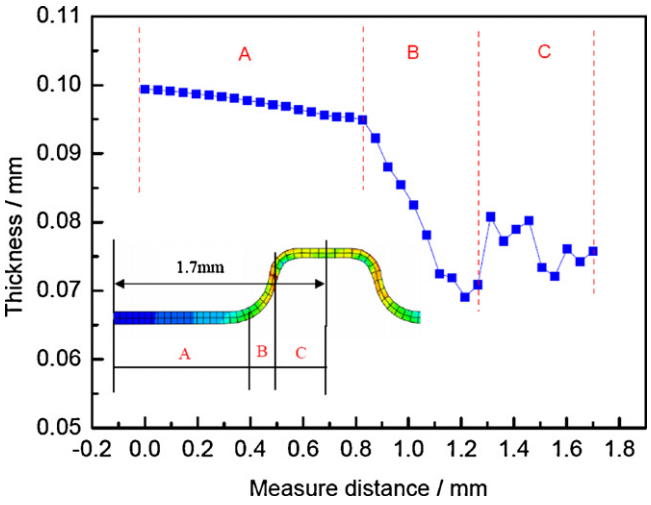

Fig. 13. Thickness variation of the formed plate.

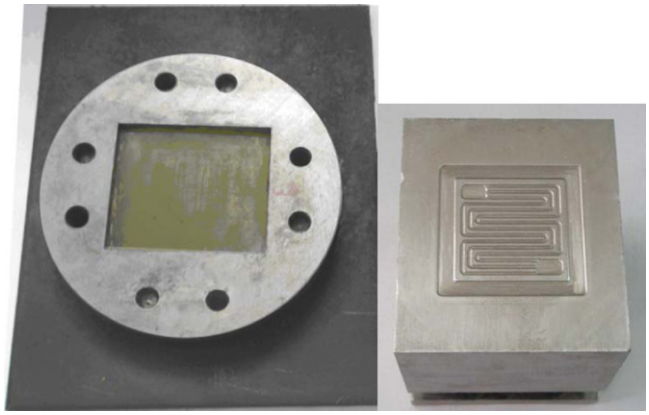

Fig. 14. Photographs of the forming equipment for the experiment.

an important factor in the forming process because the rubber pad is enclosed in the container, incompressible during the deformation, and capable of transferring the same loading force regardless of hardness.

3.6.4. Thickness variation

During the forming process, the thickness of the formed plate will decrease. However, after deformation, the thickness distribution of the three micro-channels is almost the same. Moreover, the thickness distribution of one channel is symmetrical. In this study, we are most concerned with the rupture region within half of one channel. Therefore, one half of a channel of the formed bipolar plate with a length of 1.7 mm is analyzed (Fig. 13). The curve of the thickness variation as a function of the measure distance can be divided into three regions. In region A, the thickness reduction is small. In region B (the side of the micro-channel), the thickness of the blank decreases rapidly, and the thinnest point of the plate is in this region. This thin region is where the blank experienced more resistant friction force, which blocked the flow of material during the forming process. The thickness distribution is not uniform in region C due to the friction between the surfaces of the rigid die and the blank.

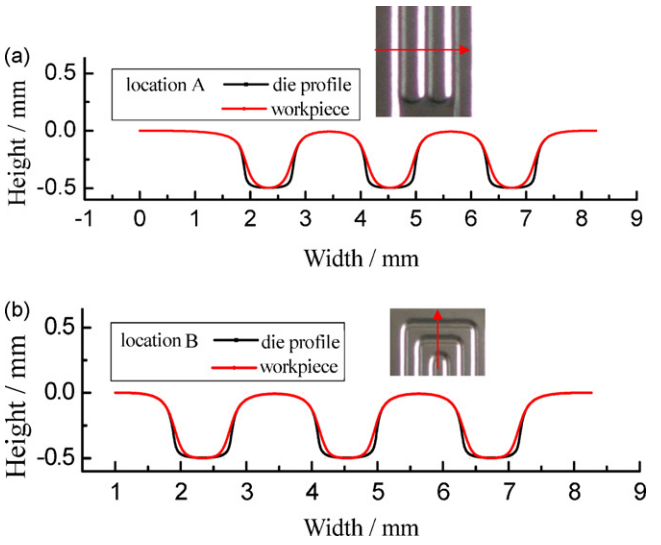

Fig. 16. Profiles of micro-channels measured by the 3D laser scanning measurement system at (a) location A and (b) location B.

4. Experimental setup

The simulation results are taken as the process parameters for the experiment. The rubber pad equipment is designed and manufactured as shown in Fig. 14, and the key geometric dimensions of the rigid die are $R = 0.3$ mm, $r = 0.2$ mm, $\alpha = 20^\circ$, and $F = 250$ kN. A polyurethane rubber with a Shore A hardness of 70 is used for the rubber pad, and an SS304 annealed stainless steel sheet

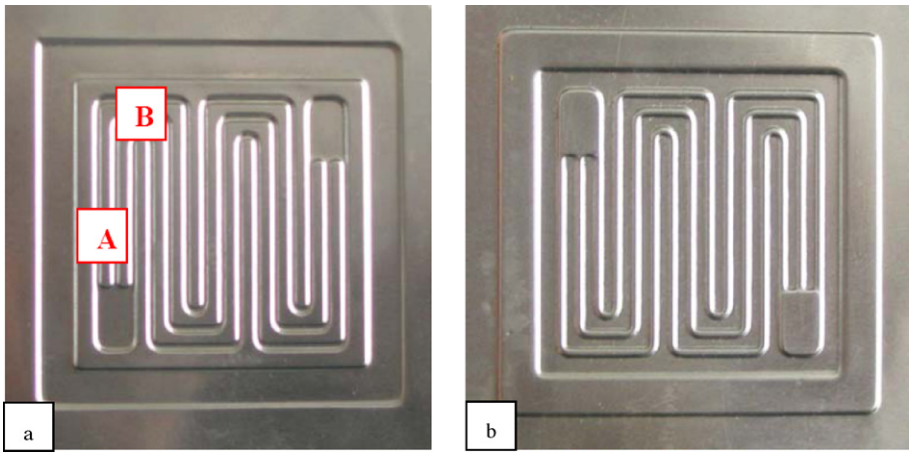

Fig. 15. (a) Front and (b) back view of a metal bipolar plate fabricated by the rubber pad forming process.

with a thickness of 0.1 mm is applied. The dimensions of the polyurethane rubber and blank are 82 mm × 75 mm × 15 mm and 82 mm × 75 mm × 0.1 mm, respectively. A hydraulic press with a capability of 1000 kN is applied.

5. Results and discussion

The metal bipolar plate samples are fabricated by rubber pad forming. The metal bipolar plate with a high surface quality is not cracked and winkled (Fig. 15).

To examine whether the blank filled the cavity of the rigid die or not, the profiles of the formed bipolar plate and the rigid die are measured using a 3D laser scanning measurement system with a measurement accuracy of 0.02 mm. A comparison of the profile at location A (vertical to the micro-channel) and location B (horizontal to the micro-channel) between the bipolar plate and rigid die is presented in Fig. 16. From this figure, it is known that the cavity of the rigid die is filled with blank very well at both location A and location B, but the load force is insufficient for the blank to fill the bottom corner of the die. The profiles of the bipolar plate and the rigid die are almost coincident, which means that the amount of spring back of the plate is very small. Based on the above analysis, it is known that the rubber pad forming process is a promising process for fabricating metallic bipolar plates.

6. Summary and conclusions

(1) This study describes the detailed procedure for the formation of a bipolar plate using the rubber pad forming process. The key process parameters of the rubber pad method are investigated with FE simulations. As the outer radius and draft angle increased, the formability of the blanks increased. The smaller the internal radius, the harder it is to fill the cavity of the rigid die. The hardness of the rubber pad is not an important parameter for the formation of a bipolar plate. The thickness distribution of the formed bipolar plate is uneven, and the most dangerous position occurred at the side of the micro-channel.

(2) A 0.1-mm thick bipolar plate of SS304 stainless steel is fabricated using rubber pad forming equipment and the optimal process parameters indicated by the FE simulation results.

(3) The formed plate had a high surface quality, and the amount of spring back of the plate is very small, indicating that the dimension precision is very high. This rubber pad forming process could improve the quality of the product because of the low stiffness of the die material and minimize the die cost. The operation of this forming process is very simple. The productivity is high, and this method can produce the plates on a large scale. Therefore, this forming process can reduce the overall cost of producing bipolar plates. The estimated cost of a double bipolar plate manufactured by this method with a non-coated SS304 is \$1.9. This cost could meet the \$6 kW^{-1} target but will be decided based on the surface treatment of the double bipolar plates. The main drawback of the rubber pad forming process is that the life of the rubber pad is not so long, and should be replaced after the production of only about 100 plates. Future studies should focus on prolonging the life of the rubber pad by changing the structure of the rigid die and the container. Overall, we strongly believe that metallic bipolar plates fabricated by the rubber pad forming process will successfully solve the problem of high fuel cell stack cost and improve the commercial competitiveness of fuel cells.

Acknowledgments

The authors would like to thank the Natural Science Foundation of China for Distinguished Young Scholars (No. 50725517) and Wuhan Academic Leader Project (No. 200750730314) for the support given to this research.

References

[1] H. Tawfik, Y. Hung, D. Mahajan, J. Power Sources 163 (2007) 755–767.
[2] N.B. Huang, B.L. Yi, M. Hou, et al., Prog. Chem. 17 (2005) 963–969.
[3] K. Sopian, Renew. Energy 31 (2006) 719–727.
[4] T. Matsuura, M. Kato, M. Hori, J. Power Sources 161 (2006) 74–78.
[5] K.S. Weil, G. Xia, Z.G. Yang, J.Y. Kim, Int. J. Hydrogen Energy 32 (2007) 3724–3733.
[6] T. Besmann, J. Henry, J. Klett, Proc. Fuel Cell Semin. 30 (2003) 61–64.
[7] L.M. Chun, T.G. Liu, J. TianJin Univ. 39 (2006) 1252–1257.
[8] M. Koc, S. Mahabunphachai, J. Power Sources 172 (2007) 725–733.
[9] S.J. Lee, C.Y. Lee, J. Power Sources 185 (2008) 1115–1121.
[10] M. Yokoyama, S. Yamaura, H. Kimura, et al., Int. J. Hydrogen Energy 33 (2008) 5678–5685.
[11] X.M. Jiang, M. Tian, J.Y. Zhang, The Application of the Polyurethane Rubber in the Field of Stamping Technology, Defense Industry Academic Press, Beijing, 1989.
[12] D.J. Browne, E. Battikha, J. Mater. Process. Technol. 55 (1995) 218–223.
[13] M.H. Dirikolu, E. Akdemir, J. Mater. Process. Technol. 148 (2004) 376–381.
[14] S. Thiruvarudchelvan, J. Mater. Process. Technol. 122 (2002) 293–300.
[15] G. Salau, Mater. Des. 22 (2001) 299–315.
[16] M. Ramezani, Z.M. Ripin, R. Ahmad, J. Mater. Process. Technol. 209 (2009) 4925–4934.
[17] U. Engel, R. Eckstein, J. Mater. Process. Technol. 125–126 (2002) 35–44.
[18] D.S. Watkins, K.W. Dircks, D.G. Epp, Novel fuel cell fluid flow field plate, US 4,988,583 [P] (1991).
[19] L.F. Peng, X.M. Lai, D.A. Liu, P. Hu, et al., J. Power Sources 178 (2008) 223–230.
[20] M.H. Dirikolu, E. Akdemir, J. Mater Process Technol. 148 (2004) 376–381.
[21] Abaqus Theory Manual, Version 6.3. Hibbitt, Karlsson and Sorensen Inc., Pawtucket, RI, USA. 2002.
[22] Z.R. Wang, Fundamentals of Plastic Deformation Mechanics, Defense Industry Academic Press, Beijing, 1989.